Excess Hydrogen Bond at the Ice-Vapor Interface around 200 K

Wilbert J. Smit,[1,*] Fujie Tang,[2,3] M. Alejandra Sánchez,[3] Ellen H. G. Backus,[3] Limei Xu,[2,4] Taisuke Hasegawa,[3,5] Mischa Bonn,[3,†] Huib J. Bakker,[1,‡] and Yuki Nagata[3,§]

[1]*AMOLF, Science Park 104, 1098 XG Amsterdam, The Netherlands*

[2]*International Center for Quantum Materials, Peking University, 5 Yiheyuan Road, Haidian, Beijing 100871, China*

[3]*Max Planck Institute for Polymer Research, Ackermannweg 10, 55128 Mainz, Germany*

[4]*Collaborative Innovation Center of Quantum Matter, Beijing 100871, China*

[5]*Department of Chemistry, Graduate School of Science, Kyoto University, Sakyoku, Kyoto 606-8502, Japan*

(Received 13 March 2017; published 28 September 2017)

Phase-resolved sum-frequency generation measurements combined with molecular dynamics simulations are employed to study the effect of temperature on the molecular arrangement of water on the basal face of ice. The topmost monolayer, interrogated through its nonhydrogen-bonded, free O-H stretch peak, exhibits a maximum in surface H-bond density around 200 K. This maximum results from two competing effects: above 200 K, thermal fluctuations cause the breaking of H bonds; below 200 K, the formation of bulklike crystalline interfacial structures leads to H-bond breaking. Knowledge of the surface structure of ice is critical for understanding reactions occurring on ice surfaces and ice nucleation.

DOI: 10.1103/PhysRevLett.119.133003

Molecular-level details of water arrangement at the surface of ice are important for a variety of disciplines: for geology, the partial and transient melting of the grain boundaries of polycrystalline ice form the origin of the plastic flow of ice masses, leading to phenomena like glacier motion and frost heave [1]; for atmospheric science, the liquidlike layer on small ice particles constitute a medium for chemical reactions [2] and determines the interaction between ice particles; and for tribology, specifically on ice surfaces [3]. For all of these phenomena and processes, knowledge of the molecular structure of the outermost water monolayer, and how that structure changes with temperature is essential.

Experimentally, probing the ice surface entails two inherent challenges. The first is that the probe should be minimally invasive, since contacting the ice surface may cause melting and nonelastic deformation of the ice surface. This can occur in force measurements such as atomic force microscopy [4,5]. Optical methods are potentially less invasive but face a second challenge: to distinguish the response of the ice surface from the response of the bulk. This problem is frequently encountered using x rays [6,7] in studying the ice surface. Since the obtained signal from the ice sample contains both bulk and interfacial contributions, it is challenging to distinguish the interfacial contribution from the total signal in an unambiguous manner. Therefore, a technique with high surface-specificity would be of great advantage to study the molecular structure of the ice surface.

Sum-frequency generation (SFG) vibrational spectroscopy constitutes a noncontact and surface-specific measurement technique and therefore is ideal for exploring the ice surface. Vibrational SFG is a second-order nonlinear optical technique involving the generation of the sum frequency of infrared and visible pulses. This process is forbidden in centrosymmetric media. As such, the centrosymmetric bulk does not contribute to the signal, making SFG surface-specific [8,9]. In addition, when the infrared light is resonant with a vibrational transition, the SFG intensity will be resonantly enhanced, allowing for probing the vibrational modes of interfacial water molecules specifically.

Previously, the surface properties of ice have been studied with homodyne-detected SFG spectroscopy [10–17] as well as SFG simulations [13,18,19]. By measuring the SFG spectra of ice with different polarization combinations of infrared, visible, and sum-frequency lights, Shen and co-workers have shown that the ice surface becomes disordered above 200 K, while it appears ordered below 200 K [16,17]. Shultz and co-workers have studied the vibrational modes of hydrogen-bonded (H-bonded) O-H groups in the range of 3200 to 3600 cm^{-1} at the ice basal surface [10,12,14,15]. Nevertheless, the measured SFG response has not been clearly connected with the structural properties of the topmost ice surface layers. For example, although a simulation study has previously predicted the presence of excess H bonds at the ice—air interface [20], this has not yet been experimentally verified.

Here, we provide insight into the molecular arrangement of the topmost surface layers at the ice-air interface by combining MD simulations with phase-resolved SFG measurements in the temperature range of 150–245 K. We observe a rather gradual transition from a clear interfacial crystalline structure at low temperature, to a more disordered surface at higher temperatures. Both the low-temperature interfacial crystalline structure and the

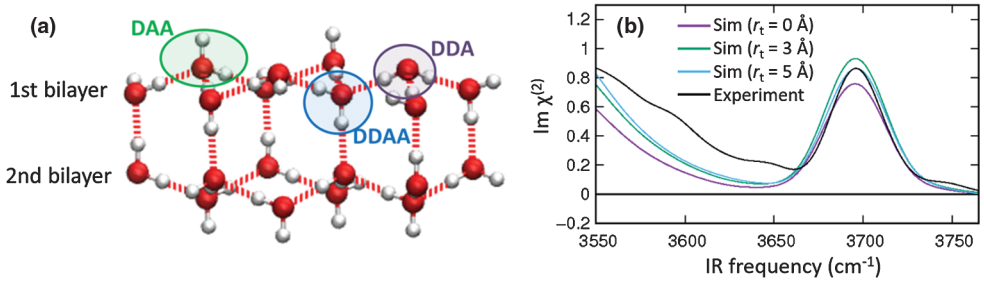

FIG. 1. (a) Schematic of the *DAA*, *DDA*, and *DDAA* water molecules at the basal ice-air interface with its perfect form. (b) Simulated SFG spectra in the free O-H region at 200 K with various cross-correlation cutoffs r_t along with the experimental result.

high-temperature structure are characterized by a reduced number of interfacial H bonds, but with very different conformations. As a result, increasing the temperature from below leads to a maximum in H-bonding density in the interfacial region around 200 K.

The preparation of single crystal ice and the experimental setup are detailed in our previous work [21]. In short, single crystalline ice was grown by seed extraction from the melt [13] and oriented between two crossed polarizers using a Rigsby stage [22]. A polished slice of 4 mm basal oriented ice was cut off and placed in a closed temperature cell which is cooled by liquid nitrogen. The SFG experiments in the O-H stretch vibrational region were performed in an *ssp*-polarization configuration indicating that the SFG and visible beams have a perpendicular polarization to the plane of incidence, while the infrared beam has a parallel polarization to the plane of incidence. Interference of the SFG signal originated at the ice surface with the SFG signal generated by a local oscillator (gold) allows for the determination of the phase-resolved *xxz* component of the second-order susceptibility $\chi^{(2)}$. The imaginary part of $\chi^{(2)}$ ($\mathrm{Im}\chi^{(2)}$) can be interpreted as a surface infrared absorption spectrum and is a sensitive probe of the molecular resonances at the ice-air surface.

Furthermore, we carried out MD simulations of the ice-air interface using a slab model. The simulation cell contains 1344 water molecules, forming 12 bilayers. Water molecules are modeled with the POLI2VS force field [23], which has been successful in simulating the SFG spectra of the liquid water-air interface [24–27]. The simulations were run in the canonical ensemble with the Nosé-Hoover thermostat. SFG spectra were generated by computing the time correlation function of the dipole moment and the polarizability [28] obtained from the POLI2VS MD trajectory. The time correlation functions were calculated by controlling the cross-correlation terms through the cutoff radius r_t within the truncated response function formalism [29]. This r_t sets the range over which the intermolecular couplings between water molecules are considered in the simulation. The relevant length scale for the intermolecular coupling is obtained when the spectrum no longer changes with increasing r_t. Details are provided in the Supplemental Material [30]. Note that SFG typically probes water molecules up to at most a few nm depth from the surface. However, here we focus on the SFG response of free O-H groups which are only present in the outermost molecular monolayer of the ice surface. As such, the spectroscopic probing depth is one monolayer in this study, but of course the spectral response of this outermost monolayer is influenced by the configuration of the deeper layers, e.g., surface reconstructions. The MD simulations account well for this influence.

Water molecules can be classified into three categories, based on the number of H bonds a water molecule donates (*D*) or accepts (*A*): *DAA* water molecules, i.e., water molecules donating one and accepting two H bonds, and, in the same notation, *DDA* and *DDAA* water molecules. These different types of water molecules are schematically depicted in Fig. 1(a). For the perfect form of the basal face, the topmost water monolayer consists of 50% *DAA* and 50% *DDA* water molecules [31]. Free O-H groups are associated solely with *DAA* molecules. However, in the range of 150–250 K, free O-H groups originate not only from *DAA* but also from *DA* water molecules with one donating and one accepting H bond. In the following, we will focus on the free O-H SFG response of the *DDA* and *DA* water molecules.

Figure 1(b) displays the simulated free O-H response at 3700 cm^{-1} at 200 K for different cutoff radii r_t together with the experimentally measured spectra. The simulated spectra are in good agreement with the experimental data. This figure further indicates that the SFG spectra simulated with $r_t = 0$, 3, and 5 Å are similar. This implies that the intermolecular vibrational coupling does not affect the free O-H stretch peak, justifying calculation of the SFG spectra with $r_t = 0$ Å to determine the temperature-dependent response.

The experimentally determined temperature dependence of the free O-H stretch $\mathrm{Im}\chi^{(2)}$ is shown in Fig. 2(a). Below 200 K, the peak position is invariant with temperature, while above 200 K it shifts to the blue with increasing temperature. These changes directly reflect a variation of the water structure at the ice interface. To understand the molecular origin of the 3700 cm^{-1} $\mathrm{Im}\chi^{(2)}$ feature at the ice-air interface in more detail, we computed SFG spectra at different temperatures with $r_t = 0$ Å. These are given in

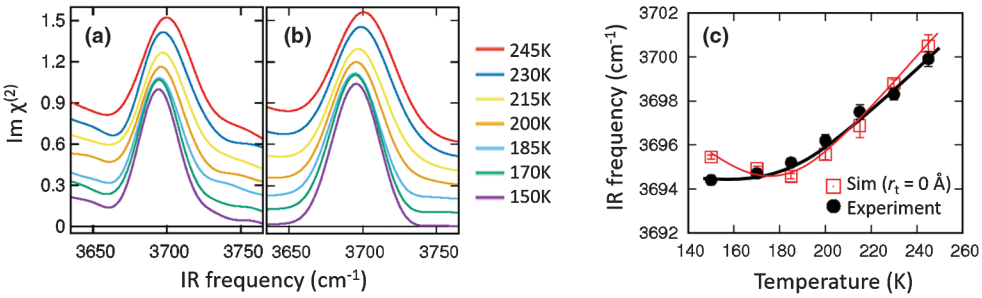

FIG. 2. Temperature dependence of (a) the experimentally measured free O-H stretch Im$\chi^{(2)}$ features; (b) the simulated Im$\chi^{(2)}$ features with $r_t = 0$ Å. The amplitudes of the peaks in the simulated spectra (b) are set to equal those in the experimental data (a). All spectra are offset by increments of 0.1 for clarity. (c) The free O-H stretch peak frequency vs temperature. The lines are to guide the eye. Error bars represent the 95% confidence intervals.

Fig. 2(b). Figure 2(c) summarizes the temperature dependence of the peak frequency in the experimentally measured and simulated SFG spectra. Both experiment and simulation data exhibit a rather similar increasing blueshift of the peak frequency with increasing temperature. The blueshift of the free O-H mode with increasing temperature is surprising, because for the liquid water-air interface the free O-H stretch mode redshifts when the temperature is increased, as is evident from MD simulations [26] and from heating effect observed in time-resolved SFG measurements [32]. A question arising here is why the peak frequency of the free O-H stretch mode of the ice-air interface is blueshifted with increasing temperature?

The blueshift of the free O-H stretch frequency may occur through the two following mechanisms. First, the free O-H frequency is affected by the frequency of the other O-H stretch mode within the same water molecule by intramolecular coupling [33]. It can be readily shown (see Supplemental Material [30]) that the change in intramolecular coupling from 150 to 245 K is responsible for at most a 1.2 cm^{-1} frequency shift, which is insufficient to account for the observed 6 cm^{-1} shift between 150 and

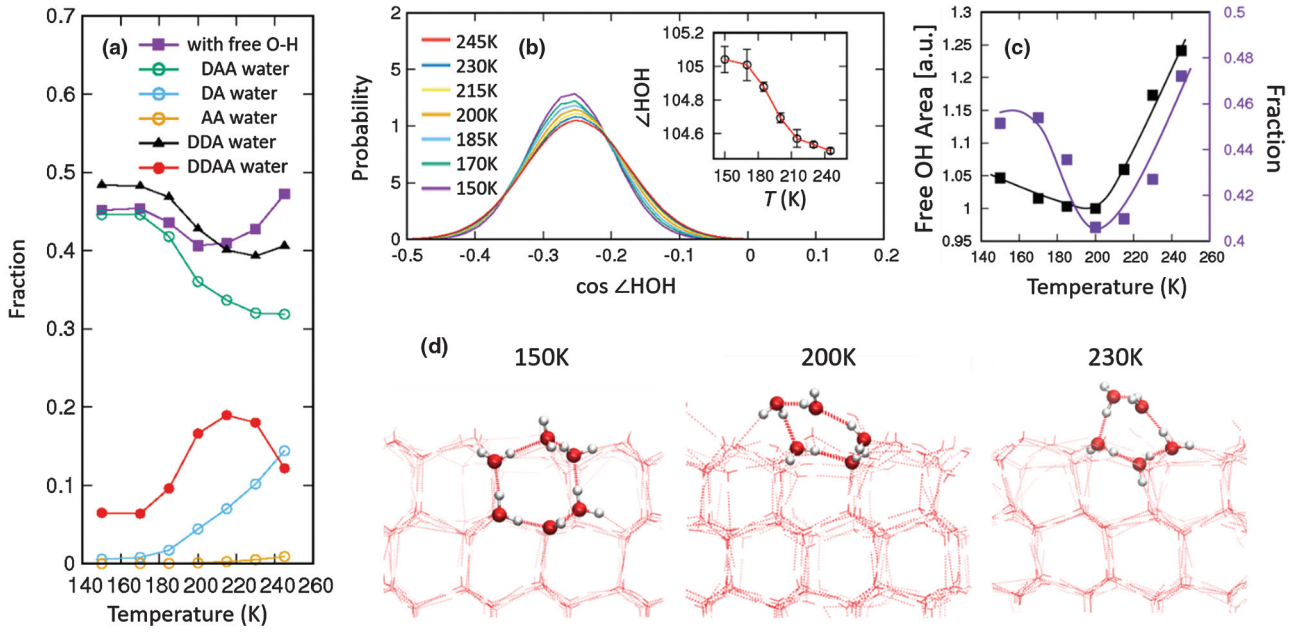

FIG. 3. (a) Simulated fraction of different interfacial water species (*DAA*, *DA*, *AA*, *DDA*, and *DDAA* water molecules) and total number of water molecules with free O-H groups (*DAA* + *DA* + *AA*) at the topmost monolayer of the ice surface. Error bars are smaller than the size of the symbols. (b) Variation of the intramolecular H-O-H angle of the DAA water molecules. The inset exhibits the H-O-H angle vs. temperature. Error bars represent 95% confidence intervals. (c) Temperature variation of the peak area of the experimentally measured free O-H SFG responses and the simulated fractions of water molecules with free O-H groups at the surface. (d) Schematics of the freezing process of ice for the basal surface of ice. This side view of the ice surface reveals that, with increasing temperature, the crystalline hexagonal structure present at 150 K starts to melt around 200 K; around this temperature the number of H-bonds is maximal, and the number of free O-H groups minimal.

245 K. Second, the free O-H frequency is determined by the number of H bonds accepted by the oxygen atom of the free O-H group [34,35]: Studies of small water clusters have revealed that the free O-H of a *DA* water molecule has a stretch frequency that is 20 cm^{-1} higher than for a *DAA* water molecule. Hence, a conversion of *DAA* to *DA*, with increasing temperature, would cause a blueshift of the free O-H stretch frequency.

To investigate whether a substantial conversion of *DAA* to *DA* occurs at the ice-air interface, we explored the interfacial composition of the water species vs temperature in the MD simulations. The result plotted in Fig. 3(a) shows that the fraction of the *DA* water molecules indeed increases dramatically with increasing temperature. Specifically, at 150 K, ~2% of the water molecules with free O-H groups ($DAA + DA + AA$ water molecules) consists of *DA* water molecules, while this fraction increases to ~30% at 245 K. Considering the frequency difference of ~20 cm^{-1} for the free O-H stretch modes of *DA* and *DAA* water molecules [34,35], a variation of the H-bond network of the water molecules with the free O-H groups indeed accounts for the observed 6 cm^{-1} shift of in the temperature-dependent SFG spectra.

Figure 3(a) reveals a second remarkable feature: up to ~200 K, the fraction of the *DAA* water molecules decreases with increasing temperature much faster than the fraction of the *DA* water increases. This means that with increasing temperature *DAA* water molecules are converted to *DDAA* water molecules, i.e., up to ~200 K, more hydrogen bonds are being formed, although the temperature is increasing.

To address the origin of this effect, we calculated the intramolecular H-O-H angle of the water molecules with the free O-H groups. Since the H-O-H angle increases by 2° when liquid water in the bulk is cooled down and converted to crystalline ice [36], it forms a good reporter for the local structure of crystalline ice. Figure 3(b) depicts the calculated temperature dependence of the H-O-H angle distribution of water molecules with free O-H groups, while the inset shows the average H-O-H angle of those water molecules vs temperature. The data illustrate that the change in H-O-H angle is accelerated below 200 K, indicating that below 200 K, the topmost ice surface increasingly starts to form a crystalline structure. When the temperature decreases below 200 K, *DDAA* water molecules in the deformed ring of the H-bond network break an H bond and form the crystal structure with the hexagonal H-bond network, thereby changing to *DAA* water molecules. As such, around 200 K, the number of free O-H groups is minimized and excess H bonds are generated, as is evident from the purple line of Fig. 3(a). The minimum number of the free O-H groups around 200 K is again fully consistent with the variation of the experimentally measured free O-H peak area, as shown in Fig. 3(c). Note that since the temperature variation of the simulated spectral area is critically affected by the quantum correction factor, a direct comparison with this area is rather arbitrary (see Supplemental Material [30]). The processes of the ice melting are summarized with the snapshots of the MD simulation in Fig. 3(d).

In summary, we have reported the temperature dependence of the free O-H SFG response of the ice Ih basal plane in both experiment and MD simulation. We show that the behavior reflects the temperature-dependent interconversion of differently hydrogen bonding-accepting and bond-donating water molecules at the ice surface. At elevated temperatures, thermal fluctuations cause breaking of hydrogen bonds; at low temperatures, the formation of crystalline interfacial structures also leads to an increase of free O-H groups at the surface. As a result, the topmost monolayer of ice has a minimum in free O-H groups and a maximum in hydrogen bonds around 200 K. These results are in particular important for understanding the dependency of the melting temperature to the size of the nanoscale ice [37] and clarify the surface-induced reorganization of the hexagonal ice to cubic ice [38] and proton ordering structure [31,39,40], as the stability of the interfacial ice structure governs the surface-induced melting and reorganization. Furthermore, the interconversion of *DAA* water to *DA* water affects the mobility of water [20]. The mobility of water governs the speed of nucleation and growth of ice [20,41–43] and is likely linked to the macroscopic properties of ice such as the friction of ice [3,44].

This work is financially supported by Max Planck Society. W. J. S. acknowledges the support from the research program of the Netherlands Organisation for Scientific Research (NWO). T. F. J. and X. L. M. acknowledge the support from NSFC (Grants No. 11290162, No. 11525520) and the National Key Research and Development Program of China (Grant No. 2016YFA0300901).

W. J. S. and F. T. contributed equally to this work.

Note added.—Recently, a heterodyne-detected SFG spectrum was measured at the ice-air interface [45].

*Present address: Laboratoire Sciences et Ingénierie de la Matière Molle, ESPCI Paris, PSL Research University, CNRS UMR 7615, 10 rue Vauquelin, 75005 Paris, France.
†bonn@mpip-mainz.mpg.de
‡bakker@amolf.nl
§nagata@mpip-mainz.mpg.de

[1] C. J. L. Wilson, Y. Zhang, and K. Stüwe, Cold Reg. Sci. Technol. **24**, 177 (1996).
[2] T. F. Kahan, J. P. Reid, and D. J. Donaldson, J. Phys. Chem. A **111**, 11006 (2007).
[3] A. M. Kietzig, S. G. Hatzikiriakos, and P. Englezos, J. Appl. Phys. **107**, 081101 (2010).
[4] H. Bluhm, T. Inoue, and M. Salmeron, Phys. Rev. B **61**, 7760 (2000).

[5] A. Döppenschmidt and H.-J. Butt, Langmuir **16**, 6709 (2000).
[6] H. Bluhm, D. F. R. a. N. K. Ogletree, C. Fadley, Z. Hussain, and M. Salmeron, J. Phys. Condens. Matter **14**, L227 (2002).
[7] A. Lied, H. Dosch, and J. H. Bilgram, Phys. Rev. Lett. **72**, 3554 (1994).
[8] Y. R. Shen and V. Ostroverkhov, Chem. Rev. **106**, 1140 (2006).
[9] M. Bonn, Y. Nagata, and E. H. G. Backus, Angew. Chem., Int. Ed. **54**, 5560 (2015).
[10] H. Groenzin, I. Li, V. Buch, and M. J. Shultz, J. Chem. Phys. **127**, 214502 (2007).
[11] V. Buch, T. L. Tarbuck, G. L. Richmond, H. Groenzin, I. Li, and M. J. Shultz, J. Chem. Phys. **127**, 204710 (2007).
[12] I. L. Barnett, H. Groenzin, and M. J. Shultz, J. Phys. Chem. A **115**, 6039 (2011).
[13] M. A. Sánchez, T. Kling, T. Ishiyama, M.-J. van Zadel, P. J. Bisson, M. Mezger, M. N. Jochum, J. D. Cyran, W. J. Smit, H. J. Bakker, M. J. Shultz, A. Morita, D. Donadio, Y. Nagata, M. Bonn, and E. H. G. Backus, Proc. Natl. Acad. Sci. U.S.A. **114**, 227 (2017).
[14] P. J. Bisson and M. J. Shultz, J. Phys. Chem. A **117**, 6116 (2013).
[15] H. Groenzin, I. Li, and M. J. Shultz, J. Chem. Phys. **128**, 214510 (2008).
[16] X. Wei, P. B. Miranda, and Y. R. Shen, Phys. Rev. Lett. **86**, 1554 (2001).
[17] X. Wei, P. B. Miranda, C. Zhang, and Y. R. Shen, Phys. Rev. B **66**, 085401 (2002).
[18] Q. Wan and G. Galli, Phys. Rev. Lett. **115**, 246404 (2015).
[19] T. Ishiyama, H. Takahashi, and A. Morita, J. Phys. Chem. Lett. **3**, 3001 (2012).
[20] G. J. Kroes, Surf. Sci. **275**, 365 (1992).
[21] W. J. Smit, F. Tang, Y. Nagata, M. A. Sánchez, T. Hasegawa, E. H. G. Backus, M. Bonn, and H. J. Bakker, J. Phys. Chem. Lett. **8**, 3656 (2017).
[22] H. W. Fairbairn and F. Chayes, *Structural Petrology of Deformed Rocks* (Addison-Wesley, Cambridge MA, 1954).
[23] T. Hasegawa and Y. Tanimura, J. Phys. Chem. B **115**, 5545 (2011).
[24] Y. Nagata, C.-S. Hsieh, T. Hasegawa, J. Voll, E. H. G. Backus, and M. Bonn, J. Phys. Chem. Lett. **4**, 1872 (2013).
[25] T. Ohto, K. Usui, T. Hasegawa, M. Bonn, and Y. Nagata, J. Chem. Phys. **143**, 124702 (2015).
[26] Y. Nagata, T. Hasegawa, E. H. G. Backus, K. Usui, S. Yoshimune, T. Ohto, and M. Bonn, Phys. Chem. Chem. Phys. **17**, 23559 (2015).
[27] J. Schaefer, E. H. G. Backus, Y. Nagata, and M. Bonn, J. Phys. Chem. Lett. **7**, 4591 (2016).
[28] A. Morita and J. T. Hynes, J. Phys. Chem. B **106**, 673 (2002).
[29] Y. Nagata and S. Mukamel, J. Am. Chem. Soc. **132**, 6434 (2010).
[30] See Supplemental Material at http://link.aps.org/supplemental/10.1103/PhysRevLett.119.133003 for Simulation protocols and supporting data including effects of intermolecular couplings and intramolecular couplings on frequency shift, calculation of frequency shifts of the free O-H stretch mode due to intramolecular vibrational couplings, discussion on consistency of our study with previous work, discussion on classical time correlation function and quantum correction factor, fraction of different interfacial water species with different H-bond definitions, and SFG spectra in the C-H stretch region.
[31] V. Buch, H. Groenzin, I. Li, M. J. Shultz, and E. Tosatti, Proc. Natl. Acad. Sci. U.S.A. **105**, 5969 (2008).
[32] K. Inoue, T. Ishiyama, S. Nihonyanagi, S. Yamaguchi, A. Morita, and T. Tahara, J. Phys. Chem. Lett. **7**, 1811 (2016).
[33] I. V. Stiopkin, C. Weeraman, P. A. Pieniazek, F. Y. Shalhout, J. L. Skinner, and A. V. Benderskii, Nature (London) **474**, 192 (2011).
[34] M. Fisher, J. P. Devlin, I. Ettischer, M. Melzer, V. Buch, J. Sadlej, J. Sadlej, V. Buch, T. Ebata, N. Mikami, and N. Haven, Science **304**, 1137 (2004).
[35] M. Miyazaki, A. Fujii, T. Ebata, and N. Mikami, Science **304**, 1134 (2004).
[36] G. S. Fanourgakis and S. S. Xantheas, J. Chem. Phys. **124**, 174504 (2006).
[37] D. Pan, L. Liu, B. Slater, A. Michaelides, and E. Wang, ACS Nano **5**, 4562 (2011).
[38] T. L. Malkin, B. J. Murray, C. G. Salzmann, V. Molinero, S. J. Pickering, and T. F. Whale, Phys. Chem. Chem. Phys. **17**, 60 (2015).
[39] D. Pan, L.-M. Liu, G. A. Tribello, B. Slater, A. Michaelides, and E. Wang, J. Phys. Condens. Matter **22**, 074209 (2010).
[40] T. Sugimoto, N. Aiga, Y. Otsuki, K. Watanabe, and Y. Matsumoto, Nat. Phys. **12**, 1063 (2016).
[41] O. Björneholm, M. H. Hansen, A. Hodgson, L. M. Liu, D. T. Limmer, A. Michaelides, P. Pedevilla, J. Rossmeisl, H. Shen, G. Tocci, E. Tyrode, M. M. Walz, J. Werner, and H. Bluhm, Chem. Rev. **116**, 7698 (2016).
[42] D. R. Haynes, N. J. Tro, and S. M. George, J. Phys. Chem. **96**, 8502 (1992).
[43] S. J. Cox, S. M. Kathmann, B. Slater, and A. Michaelides, J. Chem. Phys. **142**, 184704 (2015).
[44] A. S. de Wijn and L. G. M. Pettersson, Phys. Rev. B **95**, 165433 (2017).
[45] Y. Otsuki, T. Sugimoto, T. Ishiyama, A. Morita, K. Watanabe, and Y. Matsumoto, Phys. Rev. B **96**, 115405 (2017).